IOPscience iopscience.iop.org

Home Search Collections Journals About Contact us My IOPscience

Effects of rapid thermal annealing on the optical and electrical properties of InN epilayers

This article has been downloaded from IOPscience. Please scroll down to see the full text article.

2006 J. Phys.: Condens. Matter 18 L543

(http://iopscience.iop.org/0953-8984/18/42/L02)

View the table of contents for this issue, or go to the journal homepage for more

Download details:
IP Address: 129.252.86.83
The article was downloaded on 28/05/2010 at 14:24

Please note that terms and conditions apply.

Institute of Physics Publishing | Journal of Physics: Condensed Matter

J. Phys.: Condens. Matter **18** (2006) L543–L549 doi:10.1088/0953-8984/18/42/L02

LETTER TO THE EDITOR

Effects of rapid thermal annealing on the optical and electrical properties of InN epilayers

G W Shu[1], P F Wu[1], Y W Liu[1], J S Wang[1], J L Shen[1,6], T Y Lin[2], P J Pong[3], G C Chi[3], H J Chang[4], Y F Chen[4] and Y C Lee[5]

[1] Physics Department, Chung Yuan Christian University, Chung-Li, Taiwan, Republic of China
[2] Institute of Optoelectronic Sciences, National Taiwan Ocean University, Keelung, Taiwan, Republic of China
[3] Department of Physics, National Central University, Chung-Li 320, Taiwan, Republic of China
[4] Physics Department, National Taiwan University, Taipei, Taiwan, Republic of China
[5] Department of Electronic Engineering, Tung Nan Institute of Technology, Taipei, Taiwan, Republic of China

E-mail: jlshen@cycu.edu.tw

Received 24 August 2006
Published 5 October 2006
Online at stacks.iop.org/JPhysCM/18/L543

Abstract
We studied the optical and electrical properties of InN epilayers with rapid thermal annealing (RTA). The intensity of the photoluminescence (PL) and the carrier mobility were found to increase as the temperature of RTA was increased. We suggest that the formation of compensating acceptors (indium vacancies) after RTA is responsible for the improvement of the quality in InN. The dependence of the PL emission peak on carrier concentration provides a possible method for estimating the carrier concentration in degenerate InN.

(Some figures in this article are in colour only in the electronic version)

InN has attracted extensive attention due to its unusual physical properties and potential applications in optoelectronic devices such as light-emitting diodes, lasers, high-speed electronics, and high-efficiency solar cells [1–3]. In recent years, advanced growth techniques, such as molecular beam epitaxy (MBE) and metalorganic vapour-phase epitaxy (MOVPE), have been tried in order to grow high-quality InN. However, the growth of device-quality InN epilayers is still difficult, because of the unintentional defects or/and impurities during the epitaxial growth. Due to the low growth temperature, the high equilibrium vapour pressure of nitrogen, and the lack of suitable lattice-matched substrates, residual electron concentrations of around 10^{17}–10^{20} cm^{-3} are observed in InN [4]. The theoretical mobility calculated for InN at room temperature is as high as about 14 000 cm^2 V^{-1} s^{-1} [5]. Therefore, there appears to be room for improving the material quality of InN. Post-growth annealing is used on

[6] Author to whom any correspondence should be addressed.

 © 2006 IOP Publishing Ltd Printed in the UK

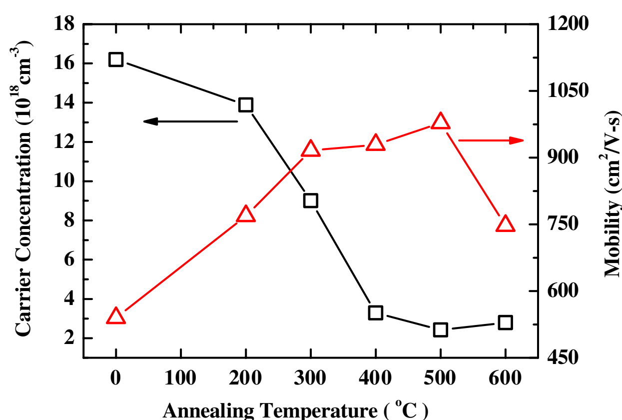

Figure 1. RTA temperature (T_{RTA}) dependence of carrier concentration and Hall mobility for InN epilayers. The lines are guides to the eye.

semiconductors to eliminate the nonradiative defects and improve sample quality. The effects of annealing on the optical properties of InN have recently been investigated [6, 7]. The annealing results in a decrease of carrier concentration as well as a redshift and a line-width narrowing of the photoluminescence (PL) band. These observations have been explained by a decrease of defects [7]. However, the detail of the mechanism for the improvement by annealing is still not very clear. Rapid thermal annealing (RTA) is known to be another effective treatment to improve the electrical and optical properties in semiconductors. The effects of RTA on nitride semiconductors have been studied recently [8]. It has been treated in GaN for activating the dopants and optimal electrical properties in the implanted layers. In addition, RTA has been used to homogenize the nitrogen composition fluctuations and reduce the grown-in nonradiative defects in GaN_xAs_{1-x}/GaAs structures [9, 10]. To date, little attention has been given to the effects of RTA on InN. Only one paper studied the morphology and surface properties of InN with high-temperature RTA [11].

In this letter, we present the effects of RTA on optical and electrical properties in InN epilayers. PL and Hall-effect measurements were employed to probe the properties of InN after RTA. It is found that the PL intensity and the carrier mobility increase as the temperature of RTA (T_{RTA}) is increased. The mechanism for the RTA-induced improvement of quality in InN is discussed.

The samples investigated were grown on sapphire substrates by metalorganic vapour phase epitaxy (MOVPE). The details of the growth method are described elsewhere [12]. Before the InN was grown, a low-temperature GaN nucleation layer was deposited, followed by growth of a GaN layer. Trimethyl-indium (TMI) and NH_3 were used as sources and N_2 was used as the carrier gas. An InN layer with a thickness of around 150 nm was grown on the GaN buffer layer. RTA treatment was performed with an annealing time of 30 s and a ramp rate of 30 °C s^{-1} at temperatures of 200, 300, 400, 500, and 600 °C. The carrier concentrations of the InN samples with different RTA temperatures were obtained from the Hall-effect measurements at room temperature, displayed as the open squares in figure 1. The electron concentration decreases as the RTA temperature (T_{RTA}) is increased. The PL measurements were performed using a pulsed diode laser operating at a wavelength of 976 nm as the excitation source. The time-integrated luminescence was collected by a spectrometer and detected using an extended InGsAs detector.

Figure 2 shows the PL spectra of InN before and after RTA. The peak intensity is substantially increased and the peak energy is shifted toward the lower energy side as T_{RTA}

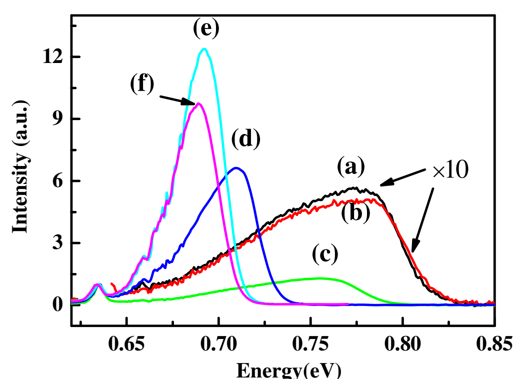

Figure 2. PL spectra of InN epilayers after RTA at 10 K: (a) as-grown; (b) RTA at 200 °C; (c) RTA at 300 °C; (d) RTA at 400 °C; (e) RTA at 500 °C; and (f) RTA at 600 °C.

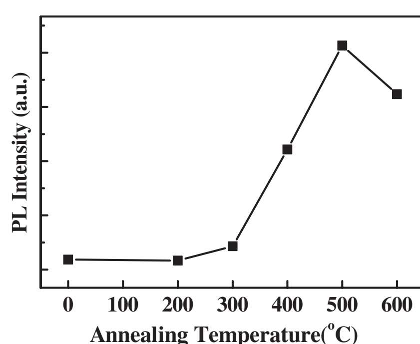

Figure 3. T_{RTA} dependence of the PL intensity for InN epilayers. The line is a guide to the eye.

is increased. Moreover, the full width at half maximum (FWHM) of PL decreases from 180 meV in the as-grown samples down to 60 meV for the InN annealed with $T_{RTA} = 500\,°C$. Figure 3 displays the PL intensity of InN after RTA, revealing a pronounced enhancement (twenty times) in the PL intensity. A similar trend has been found for the carrier mobility of InN after RTA. The open triangles in figure 1 display the carrier mobility of the InN samples versus T_{RTA}. The carrier mobility increases from 540 cm^2 V^{-1} s^{-1} in the as-grown samples up to 980 cm^2 V^{-1} s^{-1} for the InN annealed with $T_{RTA} = 500\,°C$. Apparently, the optical and electrical properties are improved with treatment of RTA. This improvement may make InN particularly useful for developing electronic and optoelectronic devices.

To investigate the effect of RTA on the structural properties of InN, scanning electron microscopy (SEM) and energy dispersive x-ray (EDX) measurements have been performed. Figures 4(a) and (b) display the SEM micrograph of InN epilayers before and after annealing at $T_{RTA} = 500\,°C$, respectively. As shown in figure 4(b), there is a ‘black region’ (local defects) visible on the micrograph for the InN with annealing at $T_{RTA} = 500\,°C$. Another black region is observed after the annealing of InN at $T_{RTA} = 600\,°C$. EDX measurements examined the black region and found that it contained a greater atomic percentage of indium than others region on the InN surface. The presence of excess indium may simultaneously correlate with some kinds of native defects in InN. We suggest that the process of RTA results in a migration of indium atoms to the black region, leading to the formation of indium vacancies (V_{In}) in the empty sites. The presence of excess indium atoms on the black region can thus be accompanied with the

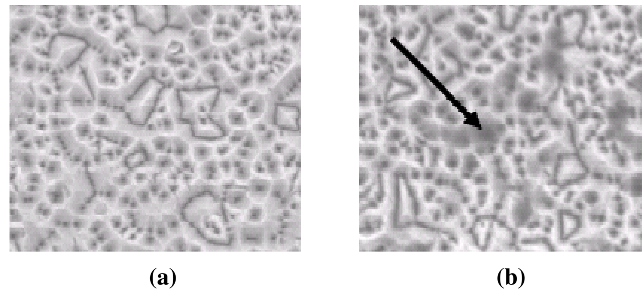

Figure 4. (a) SEM micrograph of the as-grown InN epilayers, (b) SEM micrograph of the InN epilayers annealed at $T_{RTA} = 500\,^{\circ}$C. The 'black region' is marked by the arrow.

formation of indium vacancies in other regions of the InN sample. Therefore, the concentration of indium vacancies increases as T_{RTA} increases since the black region increases with T_{RTA}. The indium vacancy formation in InN has been reported very recently [13]. The indium vacancy formation has been demonstrated to be enhanced as the growth temperature increases [13], similar to our argument. It is known that the indium and nitrogen vacancies create acceptor and donor states, respectively. If we consider that the nitrogen vacancies are the major cause of n-type conductivity in InN [1], then the decrease of the carrier concentration for InN with RTA can thus be explained by the enhanced compensation of the nitrogen and indium vacancies after the RTA. The enhancement of the PL intensity and carrier mobility for the InN after RTA is also an expected effect since the positively charged nitrogen vacancies, which act as electron scattering centres, are decreased after introducing the compensating acceptors.

The shape of the PL band in figure 2 was analysed according to the following expression [6]:

$$I(\hbar w) \sim [\hbar w]^{\gamma/2} f(\hbar w - E_g(n) - E_F), \tag{1}$$

where E_F is the Fermi energy of the degenerate electrons, n is the electron carrier concentration (expressed in cm^{-3}), $E_g(n)$ is a carrier-concentration-dependent band gap which approaches the band gap $E_g(n) \to E_g$ at vanishing concentration, f is the Fermi–Dirac function, and γ is a parameter involving the relaxation of the momentum conservation law in interband transitions ($2 \leqslant \gamma \leqslant 4$ for InN) [6]. The solid lines in figure 5 show the fitted PL spectra of InN with different T_{RTA} according to equation (1), revealing a good agreement between the fitting curves and experimental data. The agreement of the fits in figure 5 indicates that the variation of carrier concentrations is responsible for the changes of PL band for the InN after RTA. The open circles in figure 6 show the parameter $E_g(n)$ as a function of carrier concentration. It reveals a nearly linear dependence on $n^{1/3}$, in agreement with the previous result [6]. This empirical relation can be described by the following expression:

$$E_g(n) = -0.0224(n/10^{18})^{1/3} + 0.675 \text{ eV}, \tag{2}$$

plotted as a solid line in figure 6. By extrapolating $E_g(n)$ to the limit of zero electron concentration, we obtain a band gap energy of 0.675 eV for intrinsic InN. This value is within the range of the updated band gap value of 0.6–0.8 eV [14–17].

The open circles in figure 7 plot the electron concentration dependence of the PL peak energy E_{PL}. It is found that the peak energy increases as the electron concentrations increase. The PL peak energy can be estimated from the Fermi energy E_F and $E_g(n)$ [14]:

$$E_{PL} = E_F + E_g(n). \tag{3}$$

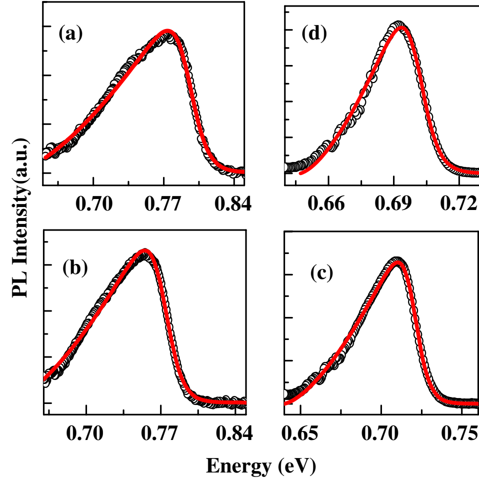

Figure 5. Measured (circles) and calculated (solid line) PL for the InN epilayers with different T_{RTA}: (a) as-grown; (b) $T_{\mathrm{RTA}} = 300\,^\circ\mathrm{C}$; (c) $T_{\mathrm{RTA}} = 400\,^\circ\mathrm{C}$; and (d) $T_{\mathrm{RTA}} = 500\,^\circ\mathrm{C}$.

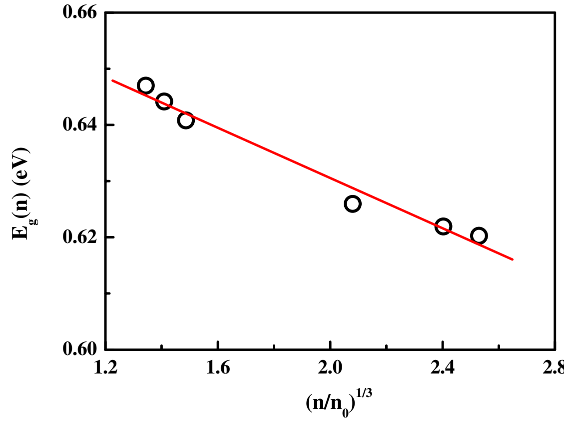

Figure 6. $E_g(n)$ as a function of carrier concentration for InN epilayers (circles). n_0 is 1×10^{18} cm^{-3}. The solid line is a fitted curve using equation (2).

By assuming an isotropic electron band, the Fermi energy E_F can be described by [15]:

$$E_F = 3.58 \left(\frac{m_0}{m_e}\right) \left(\frac{n}{10^{18}}\right)^{2/3}, \tag{4}$$

where m_0 is the free electron mass and m_e is the effective mass of an electron. Taking the value of m_e to be 0.1 m_0 [6], the concentration dependence of the PL peak energy E_{PL} calculated from equations (2)–(4) is plotted as the dashed line in figure 7. As seen from the figure, the dashed line is not appropriate to describe the concentration dependence of the PL peak energy. We attribute the discrepancy to the nonparabolicity of the conduction band since InN is a narrow band gap semiconductor. To consider the nonparabolicity effect an additional fitted term scaled as a 4/3 power of the carrier concentration has been included in the analysis:

$$E_{\mathrm{PL}} = 3.58 \left(\frac{m_0}{m_e}\right) \left(\frac{n}{10^{18}}\right)^{2/3} - 1.2 \times 10^{-27} n^{4/3} + E_g(n). \tag{5}$$

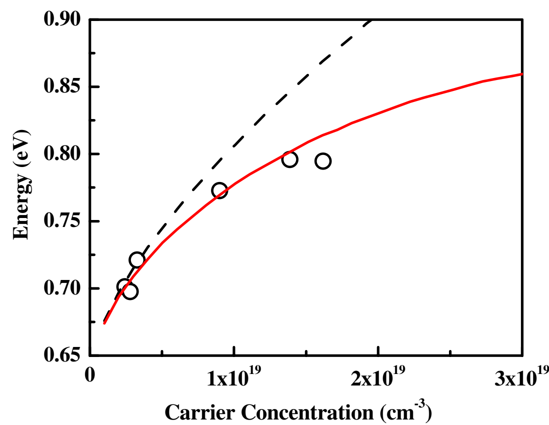

Figure 7. The measured concentration dependence of the PL peak energy (circles). The dashed line is the calculated curve according to the parabolic band. The solid line is the calculated curve with nonparabolicity correction included.

The solid line in figure 7 plots the fitted result according to equation (5), which agrees closely with the experimental results. These results demonstrate that the nonparabolicity must be taken into account in calculations of the PL peak energy for InN. Moreover, the established curve of the PL peak energy versus carrier concentration (equation (5)) provides the possibility for using the PL spectrum to estimate free carrier concentration in degenerate InN.

In summary, optical and electrical properties of the InN epilayers with RTA were investigated. The improvement of InN quality after RTA is evident from the decrease of carrier concentration as well as the increase of carrier mobility and PL intensity. These observations were explained by the formation of the compensating acceptors (indium vacancies) after RTA. The improvement of carrier mobility and PL intensity by RTA may make InN particularly useful for further development of electronic and optoelectronic devices. From the fit of the PL lineshape, we determined a band gap energy of 0.675 eV for intrinsic InN. In addition, the dependence of carrier concentration on the PL can be used to estimate the carrier concentration in degenerate InN.

This project was supported in part by the National Science Council under grant Nos NSC 94-2112-M-033-013 and NSC 94-2745-M-033-002–URD.

References

[1] Bhuiyan A G, Hashimoto A and Yamamoto A 2003 *J. Appl. Phys.* **94** 2779
[2] Butcher K S A and Tansley T L 2005 *Superlatt. Microstruct.* **38** 1
[3] Monemar B, Paskov P P and Kasic A 2005 *Superlatt. Microstruct.* **38** 38
[4] Li S X, Yu K M, Wu J, Jones R E, Walukiewicz W, Ager J W III, Shan W, Haller E E, Lu H and Schaff W J 2005 *Phys. Rev.* B **71** 161201
[5] Polyakov V M and Schwierz F 2006 *Appl. Phys. Lett.* **88** 032101
[6] Davydov V Yu, Klochikhin A A, Emtsev V V, Kurdyukov D A, Ivanov S V, Vekshin V A, Bechstedt F, Furthmuller J, Aderhold F, Graul J, Mudryi A V, Harima H, Hashimoto A, Yamamoto A and Haller E E 2002 *Phys. Status Solidi* b **234** 787
[7] Yoon J W, Kim S S, Cheong H, Seo H C, Kwon S Y, Kim H J, Shin Y, Yoon E and Park Y S 2005 *Semicond. Sci. Technol.* **20** 1608
[8] Cao X A, Abernathy C R, Singh R K, Pearton S J, Fu M, Sarvepalli V, Sekhar J A, Zolper J C, Rieger D J, Han J, Drummond T J, Shul R J and Wilson R G 1998 *Appl. Phys. Lett.* **73** 229

[9] Buyanova I A, Pozina G, Hai P N, Thinh N Q, Bergman J P, Chen W M, Xin H P and Tu C W 2000 *Appl. Phys. Lett.* **77** 2325
[10] Grenouillet L, Bru-Chevallier C, Guillot G, Gilet P, Ballet P, Duvaut P, Rolland G and Million A 2002 *J. Appl. Phys.* **91** 5902
[11] Hong J, Lee J W, Vartuli C B, Abernathy C R, Mackenzie J D, Donovan S M, Pearton S J and Zolper J C 1997 *J. Vac. Sci. Technol.* A **15** 797
[12] Shu G W, Wu P F, Lo M H, Shen J L, Lin T Y, Chang H J, Chen Y F, Shih C F, Chang C A and Chen N C 2006 *Appl. Phys. Lett.* **89** 13919
[13] Pelli A, Saarinen K, Tuomisto F, Ruffenach S and Briot O 2006 *Appl. Phys. Lett.* **89** 011911
[14] Higashiwaki M and Matsui T 2004 *J. Cryst. Growth* **269** 162
[15] Klochikhin A A, Davydov V Yu, Emtsev V V, Sakharov A V, Kapitonov V A, Andreev B A, Lu H and Schaff W J 2005 *Phys. Rev.* B **71** 195207
[16] Arnaudov B, Paskova T, Paskov P P, Magnusson B, Valcheva E, Monemar B, Lu H, Schaff W J, Amano H and Akasaki I 2004 *Phys. Rev.* B **69** 115216
[17] Carrier P and Wei S H 2005 *J. Appl. Phys.* **97** 033707